THE INTERDEPENDENCE OF CLUSTER PARAMETERS IN MIMO CHANNEL MODELING

Nicolai Czink[1,2], Ernst Bonek[1], Lassi Hentilä[3], Pekka Kyösti[3], Jukka-Pekka Nuutinen[3], and Juha Ylitalo[3,4]

[1] *Institut für Nachrichtentechnik und Hochfrequenztechnik, Technische Universität Wien, Vienna, Austria*
[2] *Forschungszentrum Telekommunikation Wien (ftw.), Vienna, Austria*
[3] *Elektrobit Testing Ltd., Oulu, Finland*
[4] *Centre for Wireless Communications (CWC), University of Oulu, Oulu, Finland*

ABSTRACT

Novel *geometry-based stochastic* MIMO channel models like the COST 273 model are using multipath clusters to model the propagation paths of the channel. Recently, we introduced a novel framework to identify and track clusters automatically. MIMO measurements from various scenarios are currently evaluated in several laboratories to parametrize the models.

From processing indoor measurements at 2.55 GHz and 5.25 GHz, we found that cluster parameters show significant correlations which have to be considered in the channel models in order to be physically relevant. In detail we observed strong positive correlation between cluster power and the number of paths within a cluster, and between all the cluster spread parameters, while we observe negative correlation between the number of clusters and the cluster spreads.

Key words: cluster-based channel modeling; MIMO; double-directional radio channel.

1. INTRODUCTION

In order to find schemes that exploit the opportunities offered by the wireless MIMO channel, MIMO channel models that are detailed yet tractable are strongly needed. A promising approach involves cluster-based MIMO channel models, like the recently published COST 273 channel model [1, 2].

Multipath clusters were initially defined as "propagation paths that show similar angles and delay", and were visually observed in measurements, e.g. by [3, 4]. Visual methods were considered as too arbitrary, moreover cluster identification for a large amount of data which comes even in multiple dimensions gets impossible.

We presented a promising *automatic* approach of identifying, tracking, and parameterizing clusters in [5], where we evaluated following parameters for each cluster individually: power, power relative to the strongest cluster, number of coexisting clusters, number of paths within the cluster, mean delay, rms delay spread, mean azimuth of arrival (AoA), rms AoA spread, mean azimuth of departure (AoD), and rms AoD spread.

Previously, correlations between these cluster parameters were introduced rather arbitrarily, e.g. in the IEEE 802.11 TGn channel model [6]. This paper shows by measurements which cluster parameters show significant correlations and how this correlation is expressed.

The rest of the paper is organized as follows: Section 2 introduces the measurement equipment and campaign. The cluster identification and parametrization framework is briefly explained in Section 3. Section 4 details the method characterizing correlations, the results are subsequently presented in Section 5. Finally, we conclude with Section 6.

2. MEASUREMENTS

2.1. Equipment

In this study we use a wideband radio channel sounder, Propsound CS$^{\text{TM}}$, which utilises periodic pseudo-random binary signals. The sounder is described in more detail in [7]. The spread spectrum signal has 100 Mchip/s chip rate and switches through all the antennas with the cycle rates presented in Table 1. Thus, sequential radio channel measurement between all possible TX and RX antenna pairs is achieved by antenna switching at both the transmitter and the receiver. The number of antenna elements used is proportional to the cycle rate. The sounder was operated in burst-mode, i.e. after four measuring cycles there was a break to allow real-time data transfer to the control laptop computer. Subsequently, we estimated the propagation paths for every snapshot in time using the ISIS$^{\text{TM}}$ (Initialisation and Search Improved SAGE) software. This estimation algorithm is based on a super-

Proc. 'EuCAP 2006', Nice, France
6–10 November 2006 (ESA SP-626, October 2006)

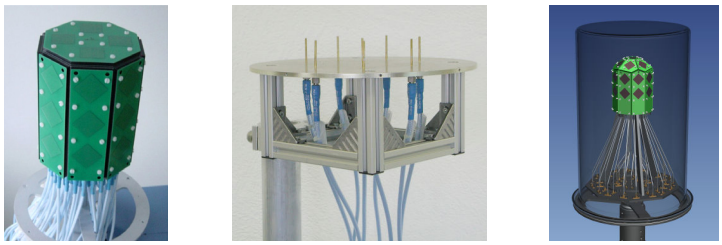

(a) 3x8 ODA, 2.55 GHz (b) 7+1 UCA, 2.55 GHz (c) 2x9 ODA, 5.25 GHz

Figure 1. Antenna arrays. (a) 2.55 GHz omni-directional patch array, (b) 2.55 GHz circular monopole array, (c) 5.25 GHz omni-directional patch array.

Table 1. Sounder parameters

Parameter	2.55 GHz	5.25 GHz
Transmit power [dBm]	26	26
Bandwidth [MHz]	200	200
Chip frequency [MHz]	100	100
Code length [μs]	2.55	2.55
Channel sampling rate [Hz]	92.6	59.4
Cycle duration [μs]	1542.24	8415.00

resolution SAGE algorithm employing maximum likelihood techniques for parameter estimation [8].

The selected antenna arrays illustrated in Figure 1 are able to capture largely the spatial characteristics of the radio channel at *both* link-ends. The 2.55 GHz array (Figure 1a) used at the TX consists of 28 dual-polarised patch elements. The elements are positioned in a way that allows channel probing in the *full* azimuth domain and almost full coverage of the elevation. Only a small cone in space angle along the supporting pole of the array cannot be covered. Figure 1b shows the uniform circular array with 7+1 monopoles used at the RX end at 2.55 GHz. It supports full azimuth direction probing but not the elevation. At 5.25 GHz both TX and RX had 25 element patch arrays shown in Figure 1c, where we used only a subset of 16 antennas at the RX. The properties of these two arrays are similar to the 2.55 GHz patch array. All antennas had been calibrated in an anechoic chamber. The signal model on which ISIS is based is using the array pattern data over rotation of the array as a base to calculate the response of each element to waves impinging from different angles.

2.2. Scenario

We took numerous measurements and decided to present results from one selected route in this paper. It is a medium-sized student laboratory (Figure 2). To facilitate comparison of results, the same routes were measured on successive measurements with different channel sounder radio modules for the two above mentioned carrier frequencies.

The measurement route changed from LOS (line of sight) to OLOS (direct line of sight obstructed by partitions, equipped with laboratory instruments), back to LOS, then

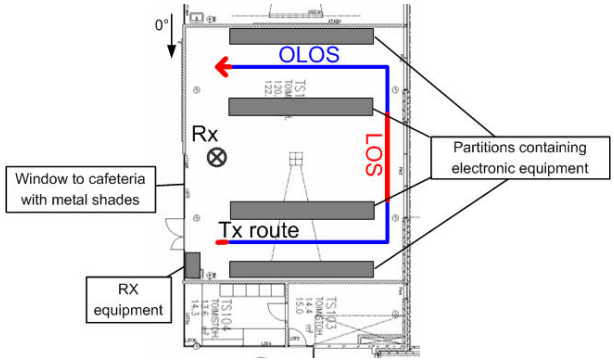

Figure 2. Measurement route in the medium-sized laboratory; Antenna orientation for 0° is the same for both Rx and Tx.

OLOS again and finished with LOS (marked with blue and red colour in Figure 2). The movement speed was around 0.5 m/s. We averaged over 4 cycles, which corresponds to 0.18λ travel for 2.55 GHz and 0.58λ for 5.25 GHz. The operation in burst mode resulted in a separation between two consecutive averaged channel estimates[1] of 0.74λ at 2.55 GHz and 2.4λ at 5.25 GHz.

3. CLUSTER IDENTIFICATION AND PARAMETRIZATION

Joint cluster identification in several dimensions, i.e. delay, AoA, and AoD, is a non-trivial task that needs sophisticated algorithms.

We presented an algorithm in [9] and improved it in [5], which is able to identify, track and parameterize clusters from MIMO channel parameter estimates. We also showed in [10] that this algorithm has physical relevance as the clusters can be mapped to real-world scattering objects.

Starting point for the clustering framework is a large number of propagation path parameters organised in

[1] We will use the term "snapshot" for indicating one averaged channel estimate in time.

snapshots estimated from the sounder impulse responses. The parameters of each path are collected in $\boldsymbol{\theta} = [\gamma\ \tau\ \varphi_{\mathrm{Tx}}\ \varphi_{\mathrm{Rx}}]^{\mathrm{T}}$, where its elements denote complex amplitude, delay, AoD, and AoA, respectively.

The clustering and validation algorithm organises the paths into an optimum number of clusters for each snapshot. Each cluster in each snapshotsis then parametrized by

$$\boldsymbol{\Theta} = [\bar{\Gamma}\ \tilde{\Gamma}\ N_p\ N_c\ \mu_\tau\ \sigma_\tau^2\ \mu_{\varphi,\mathrm{Tx}}\ \sigma_{\varphi,\mathrm{Tx}}^2\ \mu_{\varphi,\mathrm{Rx}}\ \sigma_{\varphi,\mathrm{Tx}}^2]^{\mathrm{T}},$$

where c denotes the cluster ID, and the elements of the vector denote the cluster power (in dB), the power relative to the strongest cluster during its lifetime (in dB), the number of paths within the cluster, the number of coexisting clusters, the mean delay, the delay spread, the mean AoD, the AoD cluster azimuth spread (CAS), the AoA, and the AoA CAS, respectively.

Subsequently, the clusters are tracked over several snapshots. The final outcome of the clustering framework is a number of *tracked* clusters and their parameters that existed in the radio channel during the measurement run. For our evaluations we use only clusters with lifetimes larger than one snapshot. The parameters of each tracked cluster vary slightly for each snapshot, so we use the mean values over time.

4. EVALUATION

One can expect that the cluster parameters are correlated with each other. To quantify the cross-correlation, we use two concepts, the correlation coefficients and a multi-dimensional kernel density estimate. While the correlation coefficients can *quantify* the correlation, kernel density estimates demonstrate *illustrate* how this correlation is expressed in the multi-dimensional parameter space.

4.1. Correlation coefficients

The correlation coefficients are calculated as follows[2]: If $\mathbf{C}_{\boldsymbol{\Theta}}$ is the covariance matrix, $\mathbf{C}_{\boldsymbol{\Theta}} = \mathrm{E}\{(\boldsymbol{\Theta} - \mathrm{E}\{\boldsymbol{\Theta}\})(\boldsymbol{\Theta} - \mathrm{E}\{\boldsymbol{\Theta}\})^{\mathrm{H}}\}$, then the (i,j)th element of the correlation coefficients matrix $\boldsymbol{\Phi}$ is defined as

$$\boldsymbol{\Phi}(i,j) = \frac{\mathbf{C}_{\boldsymbol{\Theta}}(i,j)}{\sqrt{\mathbf{C}_{\boldsymbol{\Theta}}(i,i) \cdot \mathbf{C}_{\boldsymbol{\Theta}}(j,j)}}.$$

This matrix is symmetric and all the diagonal elements are unity, since the power was normalized. The off-diagonal elements quantify the correlation between the respective dimensions in the range of $[-1, 1]$, where 0 denotes no correlation, and 1 (or -1) linear (counter-)dependence.

[2] $\mathrm{E}\{\cdot\}$ denotes the expectation operator

4.2. Multi-dimensional probability density function

To study the actual joint distribution of the parameters, we estimate the multi-dimensional probability density function (pdf) of the parameters using a kernel density estimator (KDE) with Gaussian kernels (implementation and more information available from [11]). All parameter vectors $\boldsymbol{\Theta}$ from the tracked clusters are used as data points to support the estimation.

The output of the KDE is an estimate of the multi-dimensional pdf $p(\boldsymbol{\Theta})$. For visualization we marginalize the pdf to two considered dimensions by integrating over the non-considered other dimensions.

5. RESULTS

In this section, we first comment on the interdependence of the cluster parameters evaluated from the measurements at a carrier frequency of 2.55 GHz, subsequently we present a comparison between 2.55 GHz and 5.25 GHz.

We applied our clustering and tracking framework to the measurement data to obtain the cluster parameter vectors $\boldsymbol{\Theta}$. Subsequently we conducted the analyses described in the previous section. To provide deeper insight, we will consider both evaluations jointly in the following.

5.1. Interdependence of cluster parameters

Figure 3a shows the correlation coefficients calculated from the measured data at 2.55 GHz according to Section 4.1, where green colour indicates no or low correlation, red colour strong correlation and blue colour strong negative correlation. Figures 4a-f depict the estimated joint pdfs.

Power ↔ relative power Figure 3 shows that the cluster power is strongly correlated with the relative cluster power (i.e. the power of the considered cluster relative to the strongest power in the snapshot). This effect is also well expressed in the estimated pdf (Figure 4a). Note that there is no full correlation between these parameters, sometimes even the strongest cluster in the snapshot is only average-powered on a global view. This is due to shadow fading. The stronger shadow fading is, the weaker this correlation will be.

Power ↔ number of paths Power is also correlated with the number of paths within a cluster. Obviously, the more paths there are within a cluster, the stronger the cluster gets. Although there is quite strong correlation, the estimated pdf in Figure 4b shows some contributions with a small number of paths but strong power. This can

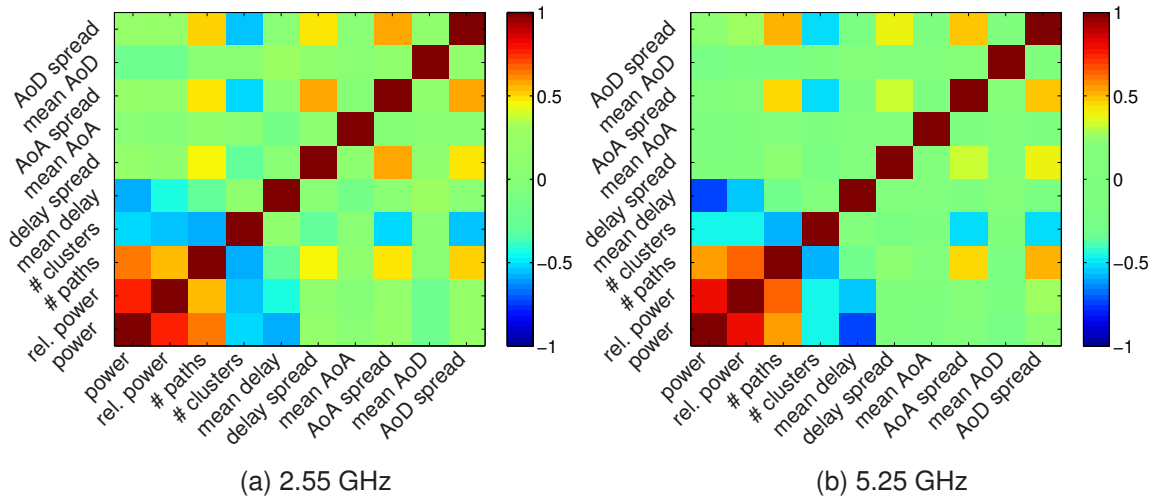

Figure 3. Correlation of cluster parameters; (a) 2.55 GHz, (b) 5.25 GHz

be attributed to clusters originating from dominant reflections, which indeed have strong power but small spreads.

Power ↔ mean delay From wave propagation it is clear that early arriving clusters carry more power than clusters with large delay. This can be observed in both Figure 3 and Figure 4c.

Cluster size: cluster delay spread ↔ AoA CAS ↔ AoD CAS The "size" of a cluster in delay and angles are described by the cluster spreads. We observe strong correlation between the CAS at the transmitter , the CAS at the receiver and the delay spread. If a cluster is "large" when seen from the Tx, it is also "large" at the Rx, so the delay spread must also be large. Figures 4e-f demonstrate this effect. We additionally observe that the distribution gets broader for larger values of the spreads. This proves that there are also few significant clusters with large delay spread but small CAS and vice-versa.

Number of clusters ↔ cluster size Representatively for the other cluster size parameters, we comment on the correlation between the number of clusters and the AoA CAS. Here, we observe a strong counter-dependence, meaning that a large number of clusters results in smaller clusters. This effect can be contributed to the cluster validation algorithm, which tries to approximate the environment with the smallest number of clusters possible. Of course, these clusters must then be larger in size.

Figure 4d, supports this explanation, but we notice that there seems to be a minimum number of 5 clusters, with a peak at 7 clusters which are necessary to describe the snapshots accurately.

5.2. Comparison of 2.55 and 5.25 GHz

We compared the results for the two carrier frequencies by using the correlation coefficients as described in Section 4.1. Figures 3a and b show the correlation coefficients of the cluster parameters. We observe very similar correlations, which are more pronounced at 2.55 GHz.

6. CONCLUSIONS

By evaluating indoor MIMO measurements, we showed that various parameters for multipath clusters are significantly correlated. This property has to be taken into account for accurate and physically relevant MIMO channel models.

Specifically we find strong correlation between (i) the cluster power and the number of paths within a cluster, (ii) all the cluster spread ("size") parameters, (iii) the number of clusters and the cluster size, and (iv) the cluster power and the cluster mean delay. Comparing the two carrier frequencies of 5.25 GHz and 2.55 GHz, we find that the correlations are quite similar, but slightly stonger expressed at 2.55 GHz.

Furthermore we showed by estimated multi-variate pdfs how the cluster parameters are correlated, which allows for straight-forward modelling of this interdependence.

ACKNOWLEDGEMENTS

We would like to thank Veli-Matti Holappa and Mikko Alatossava for the help with the measurememts. This work was conducted within the European Network of Excellence for Wireless Communications (NEWCOM). We

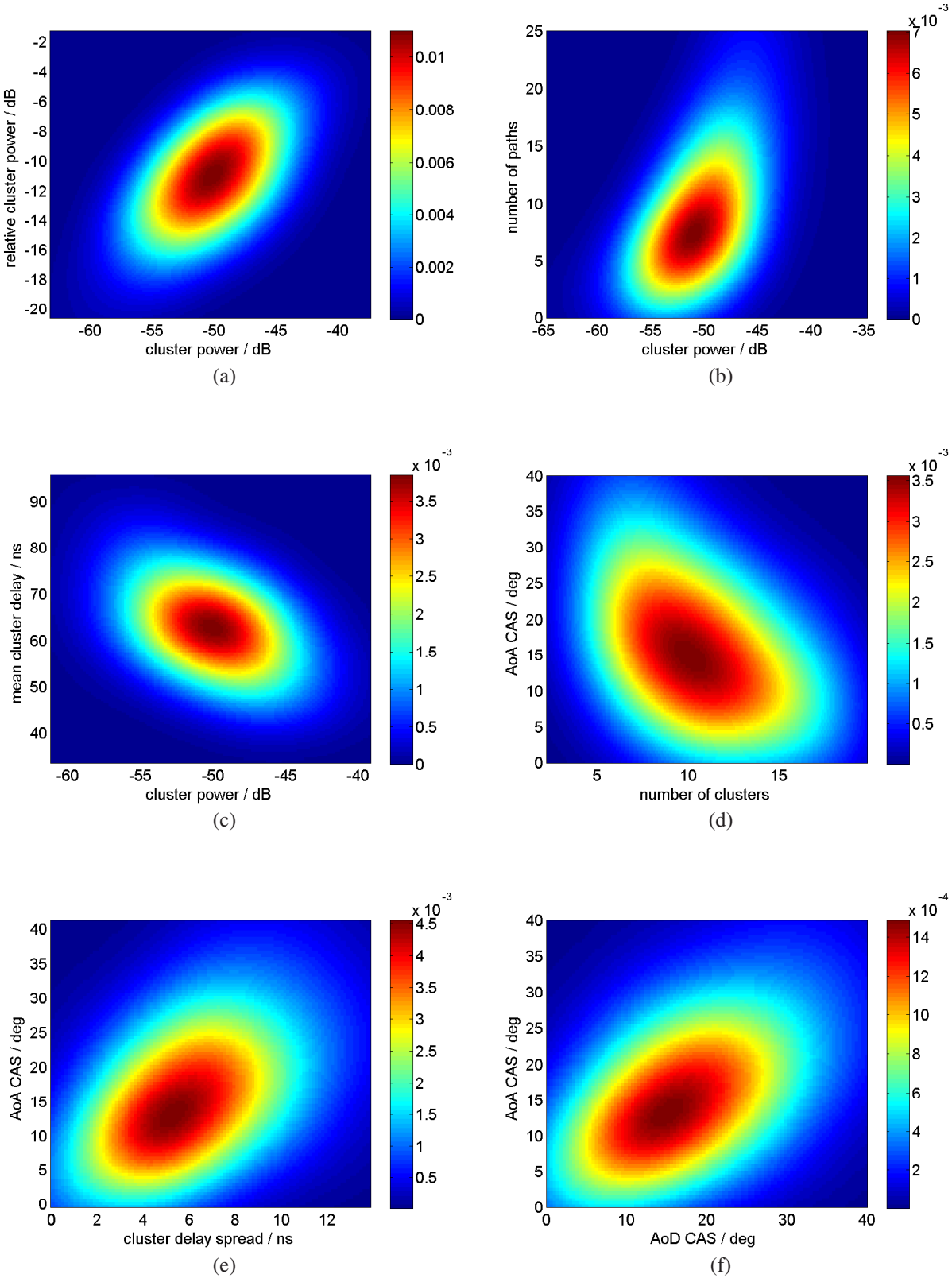

Figure 4. Estimated pdfs

thank Elektrobit Testing Ltd. for generous support. Research reported here was also supported by the Kplus program.

REFERENCES

1. L. Correia, Ed., *Mobile Broadband Multimedia Networks*. Academic Press, 2006.

2. H. Hofstetter, A. F. Molisch, and N. Czink, "A twin cluster MIMO channel model," in *European Conference on Antennas and Propagation (EuCAP) 2006*, Nice, France, 2006.

3. C.-C. Chong, C.-M. Tan, D. Laurenson, S. McLaughlin, M. Beach, and A. Nix, "A new statistical wideband spatio-temporal channel model for 5-GHz band WLAN systems," *IEEE Journal on Selected Areas in Communications*, vol. 21, no. 2, pp. 139 – 150, Feb. 2003.

4. K. Yu, Q. Li, D. Cheung, and C. Prettie, "On the tap and cluster angular spreads of indoor WLAN channels," in *Proceedings of IEEE Vehicular Technology Conference Spring 2004*, Milano, Italy, May 17–19, 2004.

5. N. Czink, E. Bonek, L. Hentilä, J.-P. Nuutinen, and J. Ylitalo, "Cluster-based MIMO channel model parameters extracted from indoor time-variant measurements," 2006, submitted to IEEE GlobeCom 2006.

6. V. Erceg *et al.*, "TGn Channel Models," IEEE P802.11 Wireless LANs, Tech. Rep., May 2004, http://www.802wirelessworld.com:8802/.

7. L. Hentilä, P. Kyösti, J. Ylitalo, X. Zhao, J. Meinilä, and J.-P. Nuutinen, "Experimental characterization of multi-dimensional parameters at 2.45 and 5.25 GHz indoor channels," in *WPMC2005*, Aalborg, Denmark, September 2005, see also http://www.propsim.com/.

8. B. Fleury, P. Jourdan, and A. Stucki, "High-resolution channel parameter estimation for MIMO applications using the SAGE algorithm," in *2002 International Zurich Seminar on Broadband Communications*, Zurich, Feb. 2002, pp. 30–1 – 30–9.

9. N. Czink, P. Cera, J. Salo, E. Bonek, J.-P. Nuutinen, and J. Ylitalo, "A framework for automatic clustering of parametric MIMO channel data including path powers," 2006, IEEE Vehicular Technology Conference 2006 Fall, accepted.

10. G. Del Galdo, V. Algeier, N. Czink, and M. Haardt, "Objects spatial localization from high-resolutino parameter estimation on measurements," 2006, accepted for publication at the NEWCOM-ACORN Workshop.

11. A. Ihler, "Kernel density estimation toolbox for matlab." [Online]. Available: http://ssg.mit.edu/ ihler/code/kde.shtml